MRT Letter: Nanoscopy of Protein Colocalization in Living Cells by STED and GSDIM

BIRKA LALKENS, ILARIA TESTA, KATRIN I. WILLIG, AND STEFAN W. HELL*
Department of NanoBiophotonics, Max Planck Institute for Biophysical Chemistry, Am Fassberg 11, 37070 Göttingen, Germany

INTRODUCTION

Far-field fluorescence microscopy is particularly important for studying the colocalization of different proteins (Tsien, 2003), which in turn is a prerequisite for mapping out protein interactions in living cells and tissues. Once limited in resolution to about half the wavelength of light (>200 nm), the recent overcoming of the diffraction barrier has boosted the versatility of fluorescence microscopy substantially (Hell, 2009; Huang et al., 2010).

In a nutshell, all current far-field fluorescence "nanoscopy" techniques of practical relevance discern neighboring features by ensuring that the fluorophores associated with these features temporarily reside in two different states (Hell, 2007, 2009): a state in which they remain dark when exposed to excitation light, and a state in which they can respond with fluorescence emission. For example, in a typical stimulated emission depletion (STED) microscope (Hell and Wichmann, 1994; Klar et al., 2000), a doughnut-shaped focal spot of the so-called STED beam is overlaid onto a regularly focused spot of an excitation beam, keeping all fluorophores exposed to the excitation beam in a dark state, except those residing close to the doughnut center (Willig et al., 2006). To this end, the wavelength and the intensity of the STED beam is adjusted such that molecules cannot assume the fluorescent state, because they are instantly forced to leave this state by de-excitation. Only molecules that happen to reside in a subdiffraction-sized region around the doughnut zero are not inhibited in their fluorescence emission. By scanning the beams across the sample, features closer than the diffraction barrier are discerned by the simple fact that they assume the fluorescent state sequentially in time.

In a stochastic single molecule switching method (Betzig et al., 2006; Hess et al., 2006; Rust et al., 2006), a single fluorophore per diffraction sized region is allowed to fluoresce stochastically in space, whereas the fluorescence of the other fluorophores remains inhibited. The emission of the fluorophore under registration is turned off again after a certain number of photons are collected on a camera that the localization of its coordinate is possible with subdiffraction precision. Applying this procedure to a representative number of fluorophores yields a subdiffraction image. While in photoactivation localization microscopy (PALM) (Betzig et al., 2006; Hess et al., 2006; Shroff et al., 2008) or stochastic optical reconstruction microscopy (STORM) (Bates et al., 2007; Rust et al., 2006) photoactivatable fluorophores are used, the concept called ground state depletion microscopy followed by individual molecular return (GSDIM) (Fölling et al., 2008; Testa et al., 2010) enables the use of many fluorophores. GSDIM employs as an on-off transition the transition between the fluorescent singlet state and a metastable dark (triplet) state which is found in basically all fluorophores. By stochastically recording in space and time (Egner et al., 2007), this approach simplified the single molecule nanoscopy methods and enabled the use of nonphotoactivatable fluorophores. Both the targeted and the stochastically switching approaches have been employed for imaging living cells using both fluorescent protein tags as well as various organic fluorophores that selectively bind to tagged

*Correspondence to: Stefan W. Hell; Department of NanoBiophotonics, Am Fassberg 11, 37070 Göttingen, Germany. E-mail: shell@gwdg.de

proteins (Fölling et al., 2008; Hein et al., 2008, 2010; Shroff et al., 2008).

Two-color (or even more color channels) nanoscopy approaches have also been carried out both in fixed (Bates et al., 2007; Bock et al., 2007; Donnert et al., 2007; Shroff et al., 2007) and living samples (Subach et al., 2010; Testa et al., 2010). However, exploiting multicolor recordings for colocalization analysis requires careful consideration of channel crosstalk and of the alignment between the different color channels. When applying stochastic methods, particular care has to be exerted on ensuring that the molecules are able to cover most of the orientation space around the z-axis to avoid mislocalizations (Engelhardt et al., 2010). Therefore, besides multicolor-imaging, approaches like Förster-resonance-energy transfer (FRET) (Jares-Erijman and Jovin, 2003; Zhang et al., 2002) and bimolecular fluorescence complementation (BiFC) are very valuable for determining the degree of colocalization of different proteins.

In BiFC a fluorescent protein such as green fluorescent protein (GFP) is split into two nonfluorescent fragments. Each of these fragments is then fused to a pair of putatively interacting proteins. The close proximity of these two proteins on interaction allows the fragments to reconstitute to a fluorescent GFP molecule (Hu et al., 2002; Kerppola, 2006). A major strength of this method is the basically background-free detection, because fluorescence is prevalent only if a GFP is reconstituted, e.g., if colocalization takes place. BiFC also requires only a very basic microscopy setup with just one excitation and one detection window, making its combination with nanoscopy by STED and GSDIM very attractive.

In this article, we demonstrate colocalization imaging at the nanoscale of tubulin and MAP2, a tubulin-associated protein, by using fluorescence complementation of the yellow fluorescent protein Citrine. Exhibiting a resolution beyond the diffraction barrier, the STED and GSDIM images demonstrate a powerful yet simple way of studying protein colocalization in living cells.

MATERIALS AND METHODS

Microscopy

Details of the STED- and GSDIM-setup for live-cell imaging have been described in detail elsewhere (Fölling et al., 2008; Hein et al., 2008). In brief, for STED microscopy, images were recorded with resonant mirror scanning (15 kHz, SC-30; EOPC, Glendale, NY) along the x-axis and stage scanning along the y-axis (P-733, Physik Instrumente, Karlsruhe, Germany). A STED beam at 595 nm was provided by an optical parametric oscillator (APE, Berlin) pumped by a femtosecond mode-locked Titanium Sapphire laser (MaiTai, Spectra Physics).

The STED focal doughnut was created by introducing a polymeric phase plate (RPC Photonics, Rochester, NY), which applies a helical phase ramp of $\exp(i\varphi)$, with $0 < \varphi < 2\pi$, in the STED beam which was then focused into a 1.4 NA objective lens (PL APO, 100x, oil, Leica, Germany). Excitation (490 nm, Picoquant, Berlin) and STED beams were overlapped and separated from the fluorescence by two custom-made dichroic mirrors. The fluorescence was filtered by a 535/50 bandpass filter and imaged onto a multimode optical fiber with an opening of the size of about an Airy disc. For imaging, the cells were transferred to a custom made sample holder using Dulbecco's modified Eagle's medium (DMEM) without phenol red as the imaging medium. All images were recorded at room temperature within 60 min after removal of the cells from the incubator.

For GSDIM, the images were recorded with a home-built setup described previously (Testa et al., 2010). The microscope was equipped with a continuous wave laser at 488 nm (Ar-Kr laser Innova 70C-5, Coherent), an oil immersion objective lens (HCX PL APO 100x/1.4 oil, Leica, Germany) for creating an $\sim$12 μm large excitation spot, and with epi-detection on an EM-CCD camera (IXON DU-897, Andor Technology, Belfast, Northern Ireland). Image analysis was performed as described before.

Cell Culture

Vero cells were cultured in DMEM supplemented with 5% FCS, 100 units/mL streptomycin/penicillin (all GIBCO-Invitrogen), and 1 mM pyruvate (Sigma) at 37°C and 5% CO_2. Twenty-four hours after seeding the cells on cover glass, they were transfected with endotoxin-free DNA by using Nanofectin (PAA) according to the manufacturer's instructions, using 3 μg of DNA for single transfections and 2 μg each for double transfections. The cells were incubated for at least 24 h before imaging.

DNA Construction

For cloning, standard methods were used. For constructing the split-Citrine-fragments for C-terminal tagging, polymerase chain reaction (PCR) using the primers GGATCGATATCGAATTCACCATGGTGAGC AAGGGCGAGGAGCTG and ATGATCCTGGCGCGCC GATGTTGTGGCGGATCT (Citrine-N172) or GGATC GATATCGAATTCACCATGGAGGACGGCAGCGTGCA GC and ATGATCCTGGCGCGCCCTTGTACAGCTCGT CCATG (Citrine-C173) were performed on a Citrine-encoding plasmid. In the plasmid pSEMS-26m-GATEWAY (Covalys), the SnapTag-sequence was substituted with the respective fragments by digestion with EcoRV and AscI and ligation. For N-terminal tagging, the PCR primer were GATCCACCGGTATGGTGAGCAA GGGCGAGGAGCTG and ATGATCCTCTTAAGTTA-GATGTTGTGGCGGATC (Citrine-N172) or GATCCA CCGGTGAGGACGGCAGCGTGCAGC and ATGATCC TCTTAAGTTACTTGTACAGCTCGTCCATG (Citrine-C173). AgeI and AflII digestion was used for substituting Snap26m in pSEMS-GATEWAY-26m (Covalys).

Abbreviations:

BiFC, bimolecular fluorescence complementation; DMEM, Dulbecco's modified Eagle's medium; FRET, Förster-resonance-energy transfer; GFP, green fluorescent protein; GSDIM, ground state depletion microscopy followed by individual molecular return; PALM, photoactivation localization microscopy; PCR, polymerase chain reaction; STED, stimulated emission depletion; STORM, stochastic optical reconstruction microscopy.

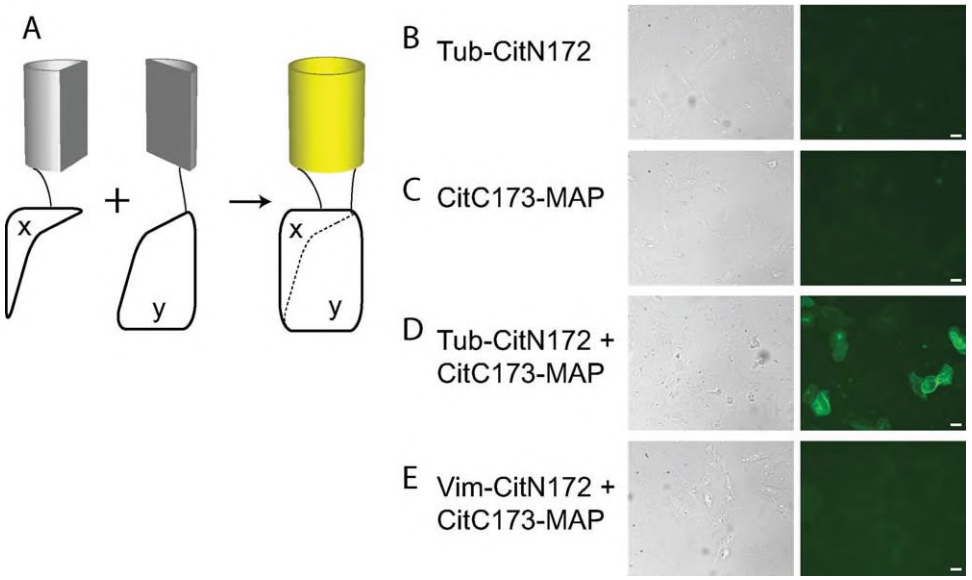

Fig. 1. **A**: Principle of bimolecular fluorescence complementation. Two nonfluorescent fragments of a fluorescent protein are fused to protein x and y, respectively. Only if x and y are in close proximity, e.g., forming a complex xy, the two fragments can restore a functional (fluorescent) protein. B–E: Microscopic images of different splitCitrine-constructs: Both N-terminal and C-terminal fragment fusion proteins expressed alone do not fluoresce on blue illumination (**B**, **C**). Only if these two fragments are expressed together as fusion proteins of interacting proteins (here: tubulin and MAP2), fluorescence is restored (**D**). If fusion proteins of two noninteracting proteins like MAP2 and Vimentin are coexpressed, no fluorescence can be observed (**E**). Scale bars = 20 μm.

Similarly, the whole fluorescent protein Citrine was introduced into these plasmids. Gateway vector conversion was used for creating the plasmids Citrine-N172-MAP2, α-tubulin-Citrine-C173, Citrine-MAP2 and α-tubulin-Citrine.

RESULTS

We studied the colocalization of the microtubule-associated protein MAP2 with α-tubulin using BiFC. Citrine is known to be viable for live-cell nanoscopic imaging, offering a resolution down to 50 nm in living mammalian cells (Fölling et al., 2008; Hein et al., 2008). Therefore, we chose Citrine as the fluorescent protein for the BiFC. Nanoscopic images in living mammalian cells were obtained using both the coordinate-targeted STED and the stochastic on-off switching GSDIM approach.

For complementation analysis, we examined the tubulin-cytoskeleton. Several proteins bind to polymerized tubulin to regulate the stability of the microtubules. A prominent example is MAP2 (microtubule-binding protein 2), which has been shown to colocalize with tubulin *in vitro* (Dehmelt and Halpain, 2005).

Citrine can be split at position 172/173, yielding a 172-amino-acid N-terminal fragment (Citrine-N172) and a 58-amino-acid C-terminal fragment (Citrine-C173), each showing negligible fluorescence on its own but the fluorescence is restored if fused to two interacting proteins(Shyu et al., 2006). To image the interaction of these two proteins in living cells with nanoscopic resolution, plasmids were constructed encoding for a N-terminal fusion of Citrine-N172 to MAP2 (CitN172-MAP2) and a C-terminal fusion of Citrine-C173 to α-tubulin (Tub-CitC173). The two fragments Citrine-C172 and Citrine-N173 complement and therefore restore fluorescence only if their respective fusion proteins are in close proximity due to any kind of interaction.

Figure 1 shows widefield-images of fixed Vero cells transfected with a combination of different Citrine-fragment encoding plasmids. As can be inferred from Figures 1B and 1C, the fragments themselves are hardly fluorescent when expressed in mammalian cells. Only on coexpression of CitN172-MAP2 and Tub-CitC173, the two fragments can restore a functional fluorescent protein, leading to a signal where the two colocalizing proteins are located (Fig. 1D). Interaction of the split-Citrine-fragments is dependent on close spatial contact. If two noninteracting proteins are tagged with two complementary fragments, such as tubulin and vimentin, no fluorescence signal can be observed (Fig. 1E). Therefore, BiFC of Citrine is a convenient tool for investigating the specific interaction of proteins.

Next, we recorded STED images of these samples. For comparison, we also imaged the single fusion proteins tubulin-Citrine and Citrine-MAP2. Figure 2 shows fluorescence images of the Citrine-labeled tubulin-cytoskeleton of a living mammalian Vero cell. In Figure 2A, α-tubulin is directly labeled with Citrine. Comparison of the confocal (left) with the STED (right) images shows the superior level of detail in the latter. All filaments can be resolved by STED microscopy, which is not the case in the corresponding confocal image, as can be easily inferred from the magnified view given in the panels. Excitation was performed with 490 nm at a repetition rate of 80 MHz and an average power of 4 μW in the lens aperture. The STED

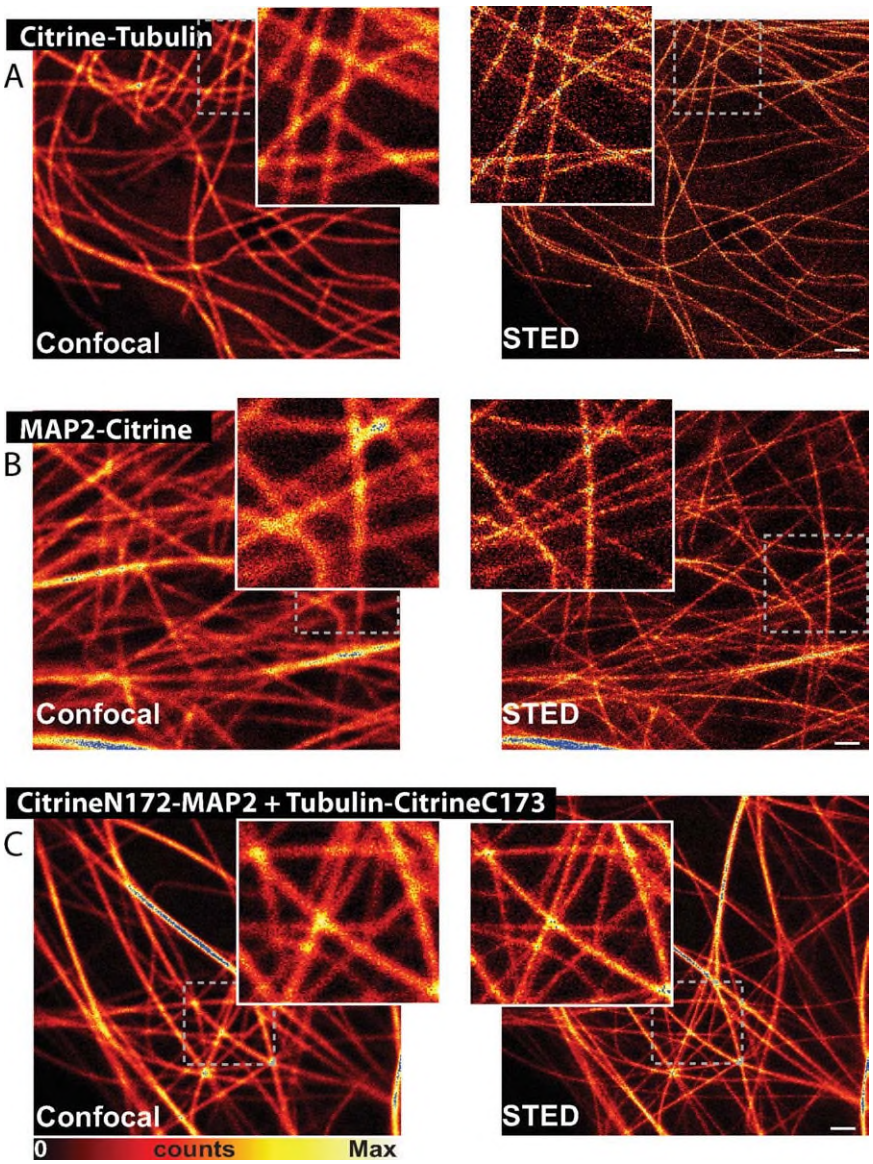

Fig. 2. Nanoscopy of the microtubular network of living mammalian cells by STED. Microtubules were labeled either directly by a Citrine-tubulin-fusion (top panel) or indirectly by Citrine-labeling the microtubule-associated protein MAP2 (middle panel). In both cases, a substantial resolution increase in the STED images (right panels) compared with the confocal images (left panels) is observed. Colocalization of MAP2 and Tubulin is examined with STED using split-Citrine (bottom panel): an N-terminal Citrine-fragment fused to tubulin was coexpressed with a C-terminal Citrine-fragment fused to MAP2, leading to fluorescence at sites of colocalization. In the STED image, a similar resolution increase as for the directly labeled structures is visible. Scale bars = 1 μm.

beam (595 nm) average power was 24 mW, which allows one to calculate a resolution <65 nm in the focal plane of the sample.

Figure 2B shows images of a Vero-cell expressing MAP2 labeled with Citrine. Again, the tubulin-cytoskeleton is much more clearly resolved in the STED-image, revealing important details of the fine structure. The settings were similar to the ones described above.

For examining the colocalization of MAP2 and α-tubulin, we double-transfected Vero cells with CitN172-MAP2 and Tub-CitC173 (Fig. 2C). As can be deduced from the comparison with Figures 2A and 2B, the distribution of the reconstituted fluorophores shows a similar structure as the tubulin cytoskeleton, confirming that α-tubulin and MAP2 colocalize in living mammalian cells (Dehmelt and Halpain, 2005). In the STED-image, the resolution is substantially improved over its confocal counterpart, showing the viability of studying colocalization of different proteins in living cells at the nanoscopic level by using fluorescence complementation. Importantly, a similar resolution enhancement is obtained as for STED imaging using plain Citrine.

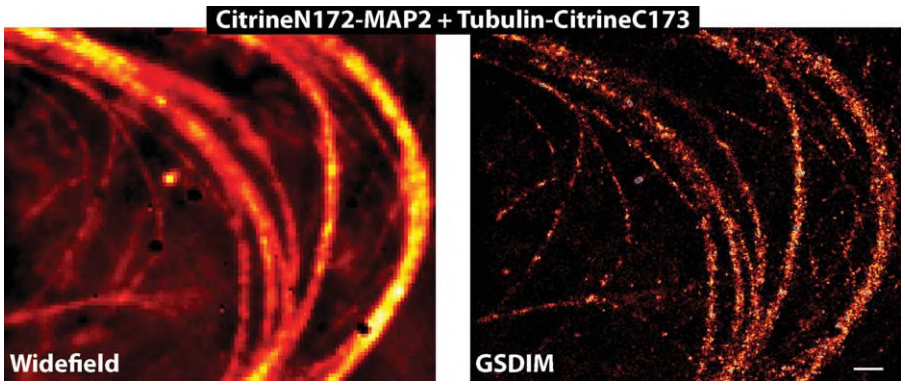

Fig. 3. Nanoscopy of a living mammalian cell coexpressing tubulin-CitrineC173 and CitrineN172-MAP2 by GSDIM. The number of camera frames was 40,000; the camera rate was 166 Hz; 150,000 events were detected. The superior resolution of the GSDIM over the conventional epifluorescence image is clearly visible in the right panel. The conventional image (left panel) was obtained by adding up all the single molecule events detected. Scale bar = 1 μm.

In addition to the STED imaging, Citrine was also used for GSDIM imaging. Since GSDIM uses a dark metastable state for inhibiting fluorescence emission, it can also be carried out with nonphotoactivatable fluorescent proteins such as Citrine. Irradiation with UV-light is not mandatory, which is beneficial for imaging living cells. Figure 3 shows an example where (similarly to Fig. 2C) a living mammalian cell expressing splitCitrine-N172-MAP2 and tubulin-splitCitrine-C173 was imaged. Also in this case, the resolution enhancement in the GSDIM image (right) compared with the conventional widefield image (left) is easily confirmed.

DISCUSSION AND CONCLUSION

The STED and GSDIM images of splitCitrine-labeled tubulin-structures prove the viability of colocalization studies in living cells using a split fluorescent protein, with a spatial resolution beyond the diffraction limit. Our data shows that this approach opens up new possibilities for studying cellular structures and intracellular connections at a much higher level of detail than previously achieved. An advantage over multicolor-imaging is that only a single fluorophore is detected, which vastly simplifies the setup because no alignment of different channels is needed. Citrine has been extensively used for STED imaging including with continuous wave lasers (Hein et al., 2008). Since continuous wave STED microscopes have found increased use due to their commercial availability, the approach reported herein should be of widespread interest.

Further improvements in the engineering of the fragmented fluorescent proteins would help to broaden their applicability even further: To also monitor dynamics of protein interaction, an acceleration of the maturation of fragmented fluorescent proteins will be helpful. Also, the fact that the complementation is in essence nonreversible impedes the examination of transient protein interactions. Although Citrine is a state-of-the-art fluorescent protein for STED and GSDIM, further improvements in the fluorescent protein photostability should allow longer image acquisition at even higher resolution. Although not observed significantly in these experiments (Fig. 1), self-assembly of the fragments has to be ruled out as well. However, when overcoming these challenges, our approach is very powerful for mapping out protein interactions at the nanoscale.

In addition to mapping the colocalization of different proteins, this approach can also be extended to BiFC based biosensing. Recently, a maltose-sensitive splitGFP has been developed, where the fluorescence is restored on a conformational change in the maltose binding protein. This protein brings two split-GFP-fragments into close spatial proximity (Jeong et al., 2006). Also, molecular events like DNA- and RNA-binding have been revealed using BiFC (Demidov et al., 2006). Altogether, our results suggest that all these studies can be combined with far-field nanoscopic approaches such as STED or GSDIM, thus allowing the examination of a variety of events in living cells with spatial resolution at the nanoscale.

ACKNOWLEDGMENTS

The authors thank Tanja Gilat for technical assistance, Lars Kastrup and Jaydev Jethwa for critical reading of the manuscript, and Andreas Schönle for support with the software ImSpector.

REFERENCES

Bates M, Huang B, Dempsey GT, Zhuang XW. 2007. Multicolor super-resolution imaging with photo-switchable fluorescent probes. Science 317:1749–1753.

Betzig E, Patterson GH, Sougrat R, Lindwasser OW, Olenych S, Bonifacino JS, Davidson MW, Lippincott-Schwartz J, Hess HF. 2006. Imaging intracellular fluorescent proteins at nanometer resolution. Science 313:1642–1645.

Bock H, Geisler C, Wurm CA, Von Middendorff C, Jakobs S, Schonle A, Egner A, Hell SW, Eggeling C. 2007. Two-color far-field fluorescence nanoscopy based on photoswitchable emitters. Appl Phys B 88:161–165.

Dehmelt L, Halpain S. 2005. The MAP2/Tau family of microtubule-associated proteins. Genome Biol 6:204.

Demidov VV, Dokholyan NV, Witte-Hoffmann C, Chalasani P, Yiu HW, Ding F, Yu Y, Cantor CR, Broude NE. 2006. Fast complementation of split fluorescent protein triggered by DNA hybridization. PNAS 103:2052–2056.

Donnert G, Keller J, Wurm CA, Rizzoli SO, Westphal V, Schoenle A, Jahn R, Jakobs S, Eggeling C, Hell SW. 2007. Two-color far-field fluorescence nanoscopy. Biophys J 92:L67–L69.

Egner A, Geisler C, von Middendorff C, Bock H, Wenzel D, Medda R, Andresen M, Stiel A-C, Jakobs S, Eggeling C, Schoenle A, Hell SW. 2007. Fluorescence nanoscopy in whole cells by asnychronous localization of photoswitching emitters. Biophys J 93:3285–3290.

Engelhardt J, Keller J, Hoyer P, Reuss M, Staudt T, Hell SW. 2010. Molecular orientation affects localization accuracy in superresolution far-field fluorescence microscopy. Nano Lett 11:209–213.

Fölling J, Bossi M, Bock H, Medda R, Wurm CA, Hein B, Jakobs S, Eggeling C, Hell SW. 2008. Fluorescence nanoscopy by ground-state depletion and single-molecule return. Nat Methods 5:943–945.

Hein B, Willig KI, Hell SW. 2008. Stimulated emission depletion (STED) nanoscopy of a fluorescent protein-labeled organelle inside a living cell. PNAS 105:14271–14276.

Hein B, Willig KI, Wurm CA, Westphal V, Jakobs S, Hell SW. 2010. Stimulated emission depletion nanoscopy of living cells using SNAP-tag fusion proteins. Biophys J 98:158–163.

Hell SW. 2007. Far-field optical nanoscopy. Science 316:1153–1158.

Hell SW. 2009. Microscopy and its focal switch. Nat Methods 6:24–32.

Hell SW, Wichmann J. 1994. Breaking the diffraction resolution limit by stimulated-emission: Stimulated-emission-depletion fluorescence microscopy. Opt Lett 19:780–782.

Hess ST, Girirajan TPK, Mason MD. 2006. Ultra-high resolution imaging by fluorescence photoactivation localization microscopy. Biophys J 91:4258–4272.

Hu CD, Chinenov Y, Kerppola TK. 2002. Visualization of interactions among bZip and Rel family proteins in living cells using bimolecular fluorescence complementation. Mol Cell 9:789–798.

Huang B, Babcock H, Zhuang X. 2010. Breaking the diffraction barrier: super-resolution imaging of cells. Cell 143:1047–1058.

Jares-Erijman EA, Jovin TM. 2003. FRET imaging. Nat Biotechnol 21:1387–1395.

Jeong J, Kim SK, Ahn J, Park K, Jeong EJ, Kim M, Chung BH. 2006. Monitoring of conformational change in maltose binding protein using split green fluorescent protein. Biochem Biophys Res Commun 339:647–651.

Kerppola TK. 2006. Visualization of molecular interactions by fluorescence complementation. Nat Rev Mol Cell Biol 7:449–456.

Klar TA, Jakobs S, Dyba M, Egner A, Hell SW. 2000. Fluorescence microscopy with diffraction resolution barrier broken by stimulated emission. PNAS 97:8206–8210.

Rust MJ, Bates M, Zhuang XW. 2006. Sub-diffraction-limit imaging by stochastic optical reconstruction microscopy (STORM). Nat Methods 3:793–795.

Shroff H, Galbraith CG, Galbraith JA, White H, Gillette J, Olenych S, Davidson MW, Betzig E. 2007. Dual-color superresolution imaging of genetically expressed probes within individual adhesion complexes. PNAS 104:20308–20313.

Shroff H, Galbraith CG, Galbraith JA, Betzig E. 2008. Live-cell photoactivated localization microscopy of nanoscale adhesion dynamics. Nat Methods 5:417–423.

Shyu YJ, Liu H, Deng XH, Hu CD. 2006. Identification of new fluorescent protein fragments for bimolecular fluorescence complementation analysis under physiological conditions. Biotechniques 40:61–66.

Subach FV, Patterson GH, Renz M, Lippincott-Schwartz J, Verkhusha VV. 2010. Bright monomeric photoactivatable red fluorescent protein for two-color super-resolution sptPALM of live cells. J Am Chem Soc 132:6481–6491.

Testa I, Wurm CA, Medda R, Rothermel E, von Middendorff C, Fölling J, Jakobs S, Hell SW, Eggeling C. 2010. Multicolor fluorescence nanoscopy in fixed and living cells by exciting conventional fluorophores with a single wavelength. Biophys J 99:2686–2694.

Tsien RY. 2003. Imagining imaging's future. Nat Cell Biol:SS16–SS21.

Willig KI, Rizzoli SO, Westphal V, Jahn R, Hell SW. 2006. STED microscopy reveals that synaptotagmin remains clustered after synaptic vesicle exocytosis. Nature 440:935–939.

Zhang J, Campbell RE, Ting AY, Tsien RY. 2002. Creating new fluorescent probes for cell biology. Nat Rev Mol Cell Biol 3:906–918.